Nuclear Instruments and Methods in Physics Research B 269 (2011) 2605–2609

Contents lists available at ScienceDirect

Nuclear Instruments and Methods in Physics Research B

journal homepage: www.elsevier.com/locate/nimb

Anisotropic rearrangement of the substrate atoms during Ar bombardment on Pd(0 0 1) surface

Sang-Pil Kim [a,1], Byung-Hyun Kim [a,b], Haeri Kim [a,c], Kwang-Ryeol Lee [a,*], Yong-Chae Chung [b], Jikeun Seo [d], Jae-Sung Kim [e]

[a] Computational Science Center, Interdisciplinary Fusion Technology Division, Korea Institute of Science and Technology, Seoul 136-791, Republic of Korea
[b] Department of Materials Science and Engineering, Hanyang University, Seoul 133-791, Republic of Korea
[c] Department of Physics, Ewha Womans University, Seoul 120-750, Republic of Korea
[d] Department of Ophthalmic Optics, Chodang University, Muan 534-701, Republic of Korea
[e] Department of Physics, Sookmyung Women's University, Seoul 140-742, Republic of Korea

ARTICLE INFO

Article history:
Received 7 March 2011
Received in revised form 19 July 2011
Available online 26 July 2011

Keywords:
Cascade induced rearrangement
MD simulation
Pd(0 0 1) surface
Surface nanostructuring

ABSTRACT

Using a three-dimensional molecular dynamics (MD) simulation, we investigated the atomic scale rearrangement that occurs on a Pd(0 0 1) surface after energetic bombardment by Ar at room temperature. High energy Ar bombardment provoked the significant rearrangement of Pd atoms in a ballistic manner with a fourfold symmetric lateral distribution aligned along the ⟨1 1 0⟩ direction. The MD simulation of uniform Ar bombardment at normal incidence on a Pd surface reproduced the experimentally observed fourfold symmetric nano-scale surface structure. The present result supports that the ballistic rearrangement of the substrate atoms plays an important role in the ion induced surface structure evolution.

1. Introduction

Self-organized nanostructures of either dots, holes or ripples produced by bombardment of energetic ions have drawn much attention, since the ordered structures of nanoscale can be produced by relatively simple and thus cheap processes [1–6]. Conventional understanding of these phenomena is based on the Bradley–Harper model [7]. In this model, the pattern formation is mainly governed by two competing processes: the erosion of the substrate atoms which is proportional to the total energy deposited at each position as prescribed by the Sigmund theory of sputter erosion [8] and the structure relaxation via surface diffusion that can be enhanced by the ion bombardment.

Recently, it was suggested from experimental observation and molecular dynamics (MD) simulations [9–14] that diverse surface reactions other than the sputter erosion and surface diffusion are provoked by ion bombardment, and significantly contribute to the morphological evolution of the bombarded surface. An example is the MD simulations of Ar bombardment on Si surface reported by Kalyanasundaram et al. [13]. They revealed that atoms in the bombarded region are not simply sputtered away, but major part of them are either displaced or redeposited around the region, thus forming large craters at the point of impact and a heap of atoms nearby. This cascade induced rearrangement of the substrate atoms can be distinguished from the thermally activated surface diffusion in long time scale since it increases the surface area of the bombarded region and it occurs in a ballistic manner that can be simulated in typical MD time scale (a few tens ps). The MD simulations prompt the development of a new multi-scale kinetic model, which uses the 'crater function' obtained by the simulation of the ion bombardment [15–17]. These models excluded the assumption that surface height change is proportional to the net energy deposited by the ion, but considered both the sputter erosion and the rearrangement by the ion bombardment. It was reported that the new kinetic model explains key experimental observations such as the stability of smooth surface during ion bombardment and the model quantitatively agrees with the ripple amplitude saturation [16,17]. The formalism also reproduced the classical Bradley–Harper results under the appropriate simplifying assumptions [16].

Analysis of the rearranged substrate atoms such as its spatial distribution and quantitative yield per ion would be thus significant to understand the surface structure evolution by the energetic ion bombardment. In the present work, we focused on the rearrangement behavior of the substrate atoms when energetic Ar bombards a Pd(1 0 0) surface at room temperature using an empirical MD simulation technique. One of the motivations of the present work was the experimental observations by Kim et al. showing that 500 eV Ar bombardment on a Pd(1 0 0) surface resulted in a

* Corresponding author. Tel.: +82 103 720 5491.
E-mail address: krlee@kist.re.kr (K.-R. Lee).
[1] Presently at School of Engineering, Brown University, Providence, RI 02912, USA.

0168-583X/$ - see front matter © 2011 Elsevier B.V. All rights reserved.
doi:10.1016/j.nimb.2011.07.093

fourfold symmetric surface nanostructure that cannot be described by the conventional kinetic models [18]. The statistical analysis of 1000 single bombardment events showed that the distribution of the rearranged atom was found to be along ⟨1 1 0⟩ directions, resulting in the square-like distribution around the region of the bombardment. Randomly superposing the ballistic rearrangement generated the fourfold symmetric surface structures in agreement with the experimental observation.

2. Simulation procedure

We simulated the bombardment of neutral energetic Ar on Pd(0 0 1) at 300 K for a variety of angles of incidence. Even if ionic Ar was used in most experiments, we assumed that the ionic Ar can be treated as neutral energetic Ar in MD simulation because free electrons on the Pd surface will significantly diminish the ionic contribution of the reaction. The kinetic energy of the Ar atoms ranged from 0.5 to 2.0 keV. Embedded atom method (EAM) potential was employed for Pd after benchmarking the potential parameters [19,20]. Strong repulsion between Pd atoms can be induced by the energetic Ar bombardment. We thus combined the EAM potential with the Ziegler, Biersack and Littmark (ZBL) potential [21] using a switching function [20]. The interaction between Ar and Pd was described by the ZBL potential. For Ar–Ar interactions, the Born-Mayer type potential was employed [22]. Fig. 1 shows the geometry of the Ar-beam and the substrate orientation. The direction of the Ar-beam is defined by the polar angle θ with respect to the surface normal, and the azimuthal angle φ between the projection of the ion-beam on the surface and the ⟨1 0 0⟩ direction of the substrate. Polar angle ranged from 0° to 75° with two azimuthal angles, 45° and 22.5°. The size of the substrate was $30 \times 30 \times 30 a_o^3$, where a_o is the lattice constant of Pd (0.389 nm). A periodic boundary condition was adopted in both the x and y directions. The atomic positions of the bottom three layers were fixed to simulate a thick substrate. The temperature of the bottom half of the remaining layers was fixed at 300 K to play the role of a thermal bath during the Ar bombardment. All the other atoms were completely unconstrained. We used very short time step, 0.01 fs, for the first 3 ps after the Ar bombardment, because the substrate atoms would move considerably fast in the early period after the bombardment. The time step was 0.1 fs for the next 10 ps and 1.0 fs for the final 10 ps. This approach produces a sufficiently accurate description of the dynamic behavior with efficiency in the simulation. Large-scale Atomic/Molecular Massively Parallelized Simulator (LAMMPS) was used for all the simulations [23].

3. Results and discussion

Fig. 2(a) shows the typical morphology of the Pd(0 0 1) substrate after bombardment by 2.0 keV Ar at normal incidence. Color

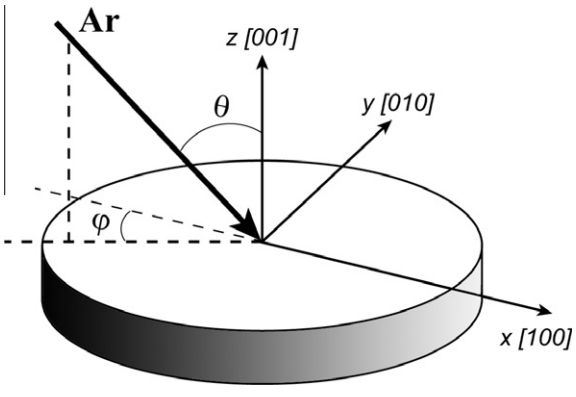

Fig. 1. The geometry of the Ar beam and the substrate orientation.

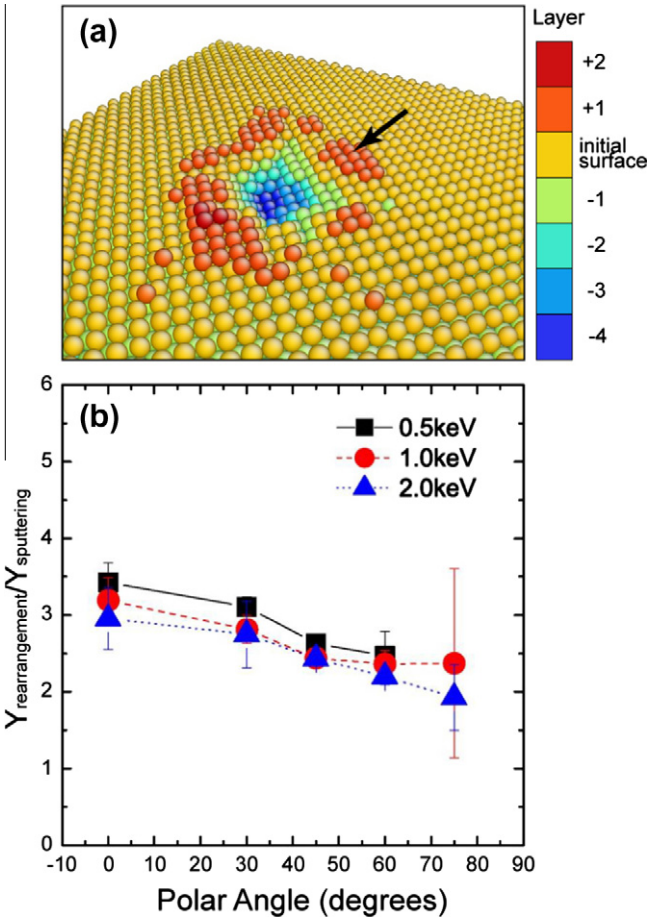

Fig. 2. (a) A snapshot of the Pd(0 0 1) surface at 2.3 ps after the commencement of normal incidence bombardment of 2.0 keV Ar at 300 K (color online). (b) Ratio of the rearrangement yield to the sputter erosion yield for various values of polar angle and the kinetic energy of Ar.

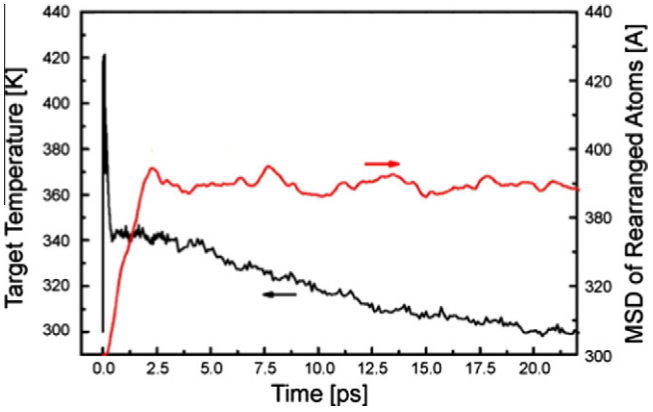

Fig. 3. The total energy change of the system and mean square displacement of the rearranged Pd atoms during the simulation of 0.5 keV Ar bombardment on the Pd(0 0 1) surface.

of the atom represents the height of the atomic position. As the energetic Ar dissipates its energy to the substrate, local melting followed by micro-explosion and rapid relaxation of the lattice atoms occurs. This surface reaction results in both the sputter-erosion and the rearrangement of the substrate atoms that generates a crater at the bombarding position and an atomic heap around

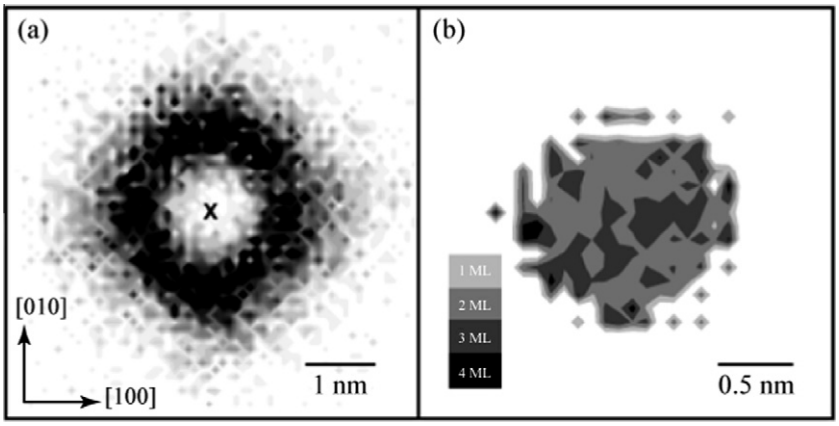

Fig. 4. The lateral distribution of the rearranged and eroded Pd atoms for Ar ions of 0.5 keV bombarding a Pd(0 0 1) surface: the lateral distribution of (a) the rearrangement for normal incidence of Ar and (b) the eroded atom position in the crater for normal incidence of Ar.

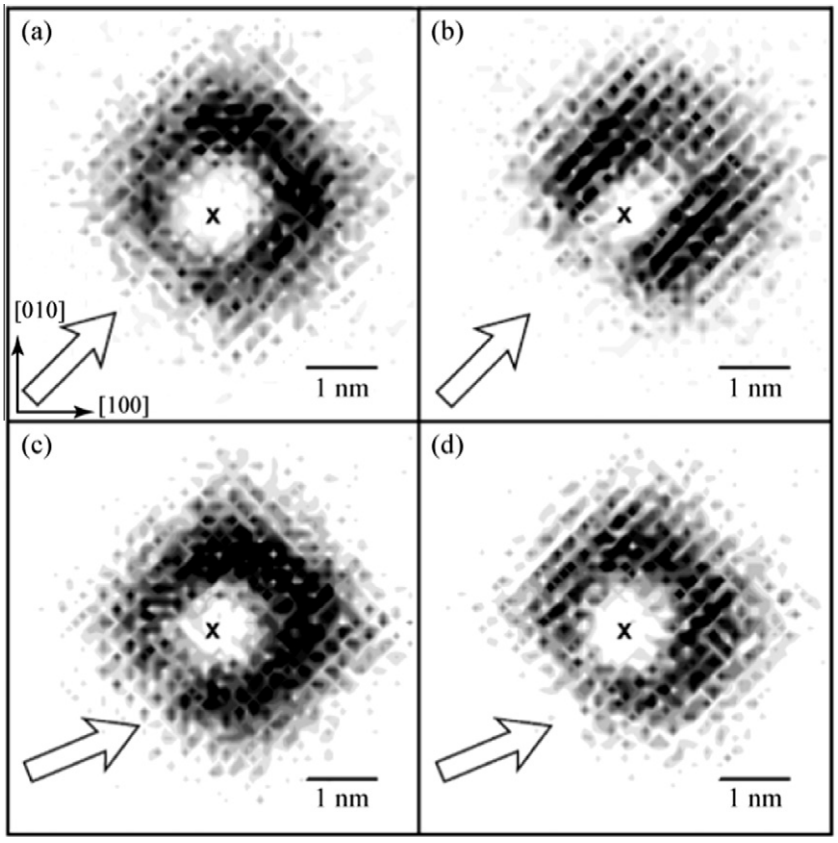

Fig. 5. The lateral distribution of the rearranged Pd atoms for Ar ions of 0.5 keV bombarding a Pd(0 0 1) surface: the lateral distribution of the rearrangement for (a) $\theta = 45°$ and $\varphi = 45°$, (b) $\theta = 60°$ and $\varphi = 45°$, (c) $\theta = 45°$ and $\varphi = 22.5°$ and (d) $\theta = 60°$ and $\varphi = 22.5°$.

the crater as indicated by an arrow in Fig. 2(a). The present observation agrees with the previous MD simulations that reported the details of the surface reaction during high-energy ion bombardment [10–13]. In this paper, we defined the rearranged atoms as those located above the initial surface after finishing the surface reaction or after 23 ps from the Ar bombardment as will be discussed in Fig. 3. Fig. 2(b) shows the ratio of the rearrangement yield to the sputtering yield for various polar angles and incidence energies of Ar. The ratio was almost independent of the incidence energy within uncertainty of the calculated yields but gradually decreased from about 3.0 to 2.0 as the polar angle increased. This result shows that the rearrangement of the substrate occurs two or three times more in abundance than the sputter erosion.

Fig. 3 shows the change in specimen temperature and the mean square displacement of the rearranged atoms when 500 eV Ar bombarded on Pd(0 0 1) surface. By depositing kinetic energy to the substrate, high temperature spike dissipated rapidly (for less than 1 ps) followed by the gradual decrease in the temperature of the specimen. The mean square displacement of the rearranged atoms showed that the rearrangement finished within 2.5 ps. Hence, it can be inferred that most of the surface processes were completed within about 2.5 ps after the Ar bombardment. After

the MD simulation for 23 ps, kinetic Monte Carlo (kMC) simulation was applied to investigate the surface diffusion in long time scale. It was hardly observed for the surface diffusion to occur at 300 K after the ballistic rearrangement.

Fig. 4(a) shows the lateral distribution of the rearranged atoms for normal incidence Ar of kinetic energy of 0.5 keV bombarding a Pd(0 0 1) surface. The distribution was obtained by collecting the distributions of 1000 independent bombardment events. The intensity of each data points is proportional to the number of the rearranged atoms. It is noted that the rearranged atoms tend to align along the ⟨1 1 0⟩ directions, resulting in a fourfold symmetric distribution. This behavior is in contrast to the rearrangement on Si (0 0 1) surface that shows an isotropic lateral distribution without resemblance to the symmetry of the substrate [13]. The difference between Pd and Si would originate from the fact that the region around the impact point of Si substrate becomes amorphous, while the metallic substrate swiftly recovers its crystallinity after each bombardment of energetic particle. It tells that the ballistic rearrangement in Pd is guided by the crystallinity of the substrate. Fig. 4(b) shows the collected distribution of the initial position of eroded atoms. In contrast to the distribution of the rearranged atoms, that of eroded atoms seems less regular, suggesting that the bond breaking and thus the distribution of the eroded atoms did not reflect the symmetry of the substrate. Instead, the rearranged atoms, approaching equilibrium to the substrate and losing their initial high kinetic energies, would diffuse preferentially along the close packed directions where the diffusion barrier is minimal, before they are stabilized to display fourfold symmetric distribution with edges along ⟨1 1 0⟩. This behavior would be also determined by the excess energy of the surface atoms. Since the atoms are mostly packed along ⟨1 1 0⟩ directions, the rearranged atoms aligned along ⟨1 1 0⟩ directions would have the lowest excess energy.

It must be noted that local incidence angle to the surface can be different from the macroscopic incidence angle as the rough surface in nanometer scale evolves. It is thus required to investigate the lateral distribution with various incidence conditions. Figs. 5(a) and (b) are the lateral distributions of the rearranged atoms when Ar bombards the surface at $\theta = 45°$ and 60° respectively with $\varphi = 45°$ (parallel to the ⟨1 0 0⟩ direction). The arrows show the projected beam directions on the surface and the y axis of the graph is in ⟨0 1 0⟩ direction. Similar fourfold symmetry was observed for $\theta = 45°$, although more atoms are displaced to the front of the ion beam. As θ increased to be 60° or with the more glancing incidence, a large fraction of the rearranged atoms were located alongside the beam direction while the number on the front and the rear sides of the incidence beam direction decreased (see Fig. 5(b)). High grazing incidence along ⟨1 1 0⟩ direction resulted in the distribution proximate to twofold symmetry, although the characteristics of square-like distribution still remained.

Figs. 5(c) and (d) show the distribution when the azimuthal angle of the incident Ar beam is in the less symmetric direction, ⟨2 1 0⟩ which corresponds to $\varphi = 22.5°$. The projection of the Ar beam trajectory on the surface is indicated by arrows in the figures. The distribution of the rearranged atoms preferentially aligned along the ⟨1 1 0⟩ direction, giving square-like patterns of the distribution as shown in Fig. 5(c) and (d). However, the rearrangement density is enhanced, most notably on the front edge of square pattern, and the maximum of the distribution is rotated from ⟨1 1 0⟩ to the incidence direction. Especially when $\theta = 60°$, the distribution with $\varphi = 22.5°$ (Fig. 5(d)) is closer to the square-like one than that with $\varphi = 45°$ (Fig. 5(b)). This enhancement seems to be caused by the fact that the incident Ar along ⟨2 1 0⟩ has shorter channeling distance than that along ⟨1 1 0⟩, and more energy dissipation of the incident Ar occurs near surface region. Similar behaviors were observed for the higher kinetic energies of the incidence Ar.

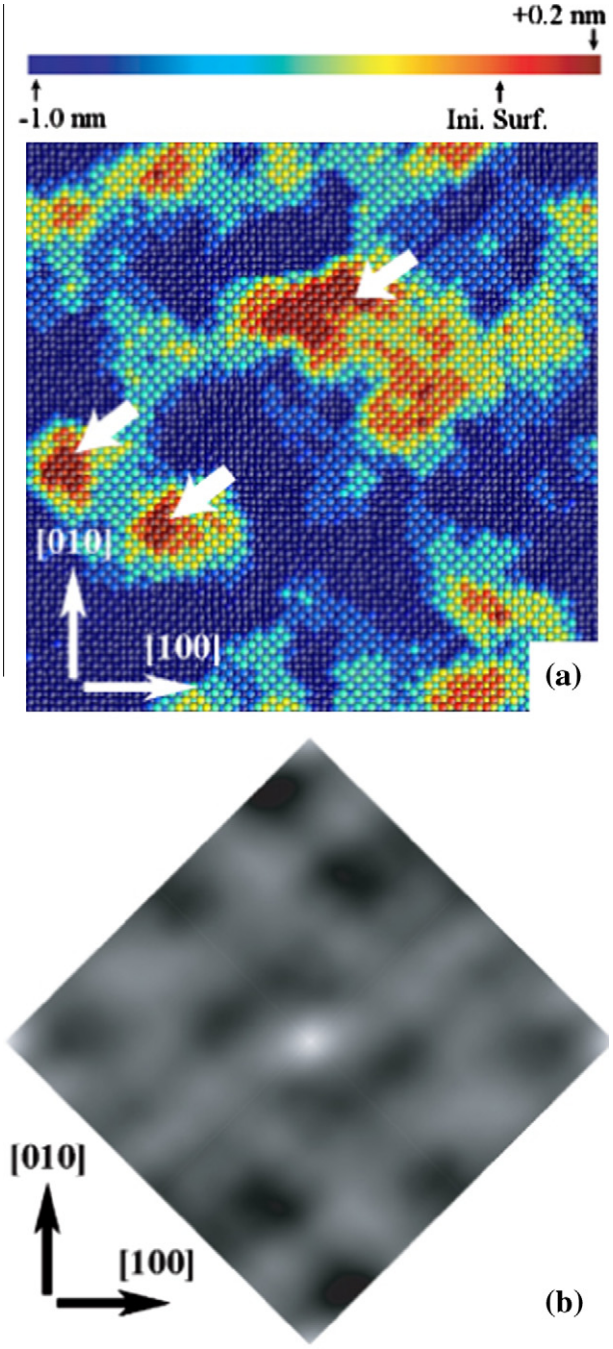

Fig. 6. (a) A snapshot of the Pd(0 0 1) surface after 4200 Ar atoms of 0.5 keV were bombarded at normal incidence at 300 K (color online). (b) The autocorrelation function of the surface shown in (a).

The statistical analysis of the simulations showed that the lateral distribution of the rearranged Pd atoms has a strong tendency to be aligned along the ⟨1 1 0⟩ direction, irrespective of the incident Ar direction. This result means that the fourfold symmetric lateral rearrangement will be retained even if the energetic Ar at macroscopically normal incidence has a different local incidence angle on a roughened surface. It should be thus interesting to examine if the local fourfold symmetric distribution of the rearranged atoms can lead to the fourfold symmetric surface nanostructures as observed in the experiment [18]. To answer the question, we simulated the morphological evolution of a Pd(0 0 1) surface at 300 K by bombarding 4200 Ar atoms of 0.5 keV at normal incidence.

The surface area of the substrate composed of 48,000 Pd atoms was $40 \times 40 a_o^2$. We adopted an acceleration method to realize the simulation because ion bombardment on the surface of area $40 \times 40 a_o^2$ is very rare in MD time scale under the real experimental condition. Simulation of the surface reaction at the experimental flux is thus impractical in terms of computation time. Each Ar atom was thus consecutively incident to the surface every 23 ps around which we found no further mass transport near the surface as shown in Fig. 3. Because no more significant surface reaction is expected after 23 ps from Ar bombardment, the present MD simulation would mimic the phenomena in real situation. Under this acceleration scheme, the flux was equivalent to $1.80 \times 10^{22}/\text{cm}^2$ s and the fluence was set to $1.74 \times 10^{15}/\text{cm}^2$. We rescaled the temperature of the system to 300 K prior to the projection of each Ar atom. Therefore, surface diffusion over long time scale was not considered in this simulation as tested by the kinetic MC simulation at room temperature. The (x, y) position of Ar incidence was randomly selected to mimic uniform Ar irradiation.

Fig. 6(a) shows the Pd surface after the bombardment of 4200 Ar atoms. Color of the surface atom represents the height of the position according to the color index bar. The snapshot of Fig. 6(a) showed that many Pd atoms are placed above the initial surface even after 4200 Ar bombardment (indicated by white arrows). The only way for the Pd atoms to be placed above the initial surface is the ballistic rearrangement caused by the energetic Ar bombardment. In the early stage of the surface structure evolution, surface nano dots are formed by the (red colored) Pd atoms agglomerated above the initial surface surrounded by the eroded region. Therefore, the present snapshot shows that the ballistic rearrangement plays a significant role in the surface structure evolution. Fig. 6(b) shows the autocorrelation function of the surface shown in Fig. 6(a). Despite the statistical noise due to the small substrate size and the low fluence, the surface features are aligned along the $\langle 1\,1\,0 \rangle$ direction with fourfold symmetry. This correlation function is comparable with the experimental results of Kim et al. who observed a fourfold symmetric nano-dot pattern on an Ar^+ ion-sputtered Pd(0 0 1) surface for normal incidence at 300 K [18], where the dots are aligned along the $\langle 1\,1\,0 \rangle$ direction.

4. Conclusions

We investigated the atomic scale rearrangement that occurs on a Pd(0 0 1) surface during the energetic Ar bombardment at room temperature using molecular dynamics simulation. It was observed in wide range of the incidence angles of energetic Ar beam that the rearrangement of Pd atoms occurs in a ballistic manner with a fourfold symmetric distribution aligned along the $\langle 1\,1\,0 \rangle$ direction. This result shows that the fourfold symmetry of the rearrangement can be maintained even when the local incidence angle varies with the surface structure evolution. The simulated Pd surface structure evolved by the uniform Ar beam bombardment of normal incidence was comparable with that of the experimentally observed fourfold symmetric nano-dots, which exposed the important contribution of the ballistic rearrangement to the surface structure evolution.

Acknowledgment

This research was supported by the Converging Research Center Program through the Ministry of Education, Science and Technology (2010K000992) and the KIST Core Capability Enhancement Program (2E21580).

References

[1] S. Facsko, T. Dekorsy, C. Koerdt, C. Trappe, H. Kurz, A. Vogt, H.L. Hartnagel, Science 285 (1999) 1551.
[2] W.L. Chan, E. Chason, J. Appl. Phys. 101 (2007) 121301.
[3] U. Valbusa, C. Boragno, F.B. de Mongeot, J. Phys.: Condens. Matter 14 (2002) 8153.
[4] M. Kalf, G. Comsa, T. Michely, Surf. Sci. 486 (2001) 103.
[5] O. Malis, J.D. Brock, R.L. Headrick, M.-S. Yi, J.M. Pomeroy, Phys. Rev. B 66 (2002) 035408.
[6] M.V.R. Murty, T. Curcic, A. Judy, B.H. Cooper, A.R. Woll, J.D. Brock, S. Kycia, R.L. Headrick, Phys. Rev. Lett. 80 (1998) 4713.
[7] R.M. Bradley, J.M.E. Harper, J. Vac. Sci. Technol. A 6 (1988) 2390.
[8] P. Sigmund, J. Mater. Sci. 8 (1973) 1545.
[9] C.M. McQuaw, E.J. Smiley, B.J. Garrison, N. Winograd, Appl. Surf. Sci. 231–232 (2004) 39.
[10] K. Nordlund, Phys. World 14 (2001) 22.
[11] E.M. Bringa, K. Nordlund, J. Keinonen, Phys. Rev. B 64 (2001) 235426.
[12] H. Gades, H.M. Urbassek, Phys. Rev. B 50 (1994) 11167.
[13] N. Kalyanasundaram, M. Ghazisaeidi, J.B. Freund, H.T. Johnson, Appl. Phys. Lett. 92 (2008) 131909.
[14] M. Moseler, P. Gumbsch, C. Casiraghi, A.C. Ferrari, J. Robertson, Science 309 (2005) 1545.
[15] B. Davidovitch, M.J. Aziz, M.P. Brenner, Phys. Rev. B 76 (2007) 205420.
[16] S. Norris, M.P. Brenner, M.J. Aziz, J. Phys.: Condens. Matter 21 (2009) 224017.
[17] N. Kalyanasundaram, J.B. Freund, H.T. Johnson, J. Phys.: Condens. Matter 21 (2009) 224018.
[18] T.C. Kim, C.-M. Ghim, H.J. Kim, D.Y. Noh, N.D. Kim, J.W. Chung, J.S. Yang, Y.J. Chang, T.W. Noh, B. Kahng, J.-S. Kim, Phys. Rev. Lett. 92 (2006) 246104.
[19] S.M. Foiles, M.I. Baskes, M.S. Daw, Phys. Rev. B 33 (1986) 7983.
[20] S.-P. Kim, S.-J. Kim, D.-Y. Kim, Y.-C. Chung, K.-R. Lee, J. Kor. Vac. Soc. 17 (2008) 81.
[21] J.F. Ziegler, J.P. Biersack, U. Littmark, The Stopping and Range of Ions in Solids, Pergamon, New York, 1985.
[22] A.A. Abrahamson, Phys. Rev. 178 (1969) 76.
[23] S.J. Plimpton, J. Comput. Phys. 117 (1995) 1.